Energy 284 (2023) 129316

Contents lists available at ScienceDirect

Energy

journal homepage: www.elsevier.com/locate/energy

A generalized equivalent circuit model for lithium-iron phosphate batteries

Antonio José Torregrosa, Alberto Broatch *, Pablo Olmeda, Luca Agizza

CMT – Motores Térmicos, Universitat Politècnica de València, Camino de Vera s/n46022, Valencia, Spain

ARTICLE INFO

Handling Editor: A. Olabi

Keywords:
Lithium-ion
Equivalent circuit models
Model order reduction
Control-oriented models
Cylindrical cells
Prismatic cells

ABSTRACT

Most of the equivalent circuit battery models available in the literature have been developed specifically for one cell and require extensive measurements to calibrate cell electrical parameters in different operating conditions. In this work, a generalized equivalent circuit model for lithium-iron phosphate batteries is proposed, which only relies on the nominal capacity, available in the cell datasheet. Using data from cells previously characterized, a generalized zeroth-order model is developed. This novel approach allows to avoid time-consuming and expensive experiments and reduces the test matrix. In spite of not relying on detailed data on the dependence of the electrical parameters with respect to state of charge, c-rate and temperature, the model provides an excellent description of the electrical behavior for both low-energy and high-energy cells, the error being always kept below 2 %. The internal resistance of the cell is expressed as a function of a new characteristic coefficient, which is typical of this lithium-ion battery chemistry. This coefficient is fitted to an exponential function of the temperature, which is physically meaningful, as the internal resistance has an Arrhenius-like behavior with respect to temperature. This model, due to its simplicity and flexibility, is particularly useful for control-oriented applications, and for off-line analyses.

1. Introduction

Lithium-ion batteries are increasingly becoming more important in the energy transition currently faced by the automotive industry [1]. This electrochemical storage system is preferable over all the other batteries because of its better power and energy density, its longer lifespan, and the almost complete absence of self-discharge effect [2]. Nonetheless lithium-ion batteries still require a lot of development and study due to some criticalities. In fact, they can work properly only in a limited range of temperatures: both for higher and lower temperatures, some issues can occur [3]. For higher temperatures, thermal runaway can lead the battery to catch fire and, in the most catastrophic cases, to explode [4]. Very low temperatures can lead to the formation of dendrites which can cause short-circuit and other problems [5]. On top of that, lithium-ion batteries can work properly only in a limited range of voltages [6]. Usually, manufacturers indicate a cut-off voltage both for charge and discharge and these limits are usually defined as minimum operating voltage (V_{min}) and maximum operating voltage (V_{max}). For voltages lower than the minimum operating voltage, some issues related to over-discharge can occur. For instance, over-discharge can lead to an increase in the gas pressure of the battery and dissolution of the electrolyte, and these phenomena can in turn lead to an increase in the battery internal resistance [7]. The over-charge, on the other hand, can lead to an uncontrollable temperature increase which can lead to thermal runaway and finally to the battery destruction [8]. All these situations are potentially dangerous for the operators. For all these reasons, it is fundamental to develop battery management systems that can opportunely control battery temperature and voltage, thus preventing the battery from working outside of the safe operation range. Battery management strategies are usually based upon control-oriented models or algorithms which can precisely and quickly provide a description of the electro-thermal behavior of the battery [9]. Models characterized by high computational cost and long computational time (electrochemical models) may not be the best choice for this kind of applications. Usually, control-oriented algorithms are based on lumped models which can describe the battery behavior by determining a few calibration parameters and providing a sufficiently precise prediction of the terminal voltage and battery temperature [10].

Equivalent circuit models are usually employed for describing the behavior of a cell [11]: a model of an entire pack can be implemented by connecting cells in series and in parallel. The literature provides numerous equivalent circuit models of lithium-ion cells, as shown by Thakkar et al. [32]. Tran et al. [12] presented a comparison of equivalent circuit models for four different chemistries (LFP, NMC, LMO, NCA).

* Corresponding author.
E-mail address: abroatch@mot.upv.es (A. Broatch).

https://doi.org/10.1016/j.energy.2023.129316
Received 27 July 2023; Accepted 7 October 2023
Available online 9 October 2023

Table 1
Climatic chamber characteristics.

Characteristic	Value
Temperature range	[-75 180] °C
Temperature fluctuation in time	< 0.3 K
Temperature variation in space	< 3.0 K
Heat up rate	4.7 K/min
Pull down rate	4.1 K/min

Table 2
Uncertainty of the variables.

Variable	Symbol	Uncertainty σ [%]
Current	I	0.33%
Voltage	v	0.1%
Temperature	T	1.68%

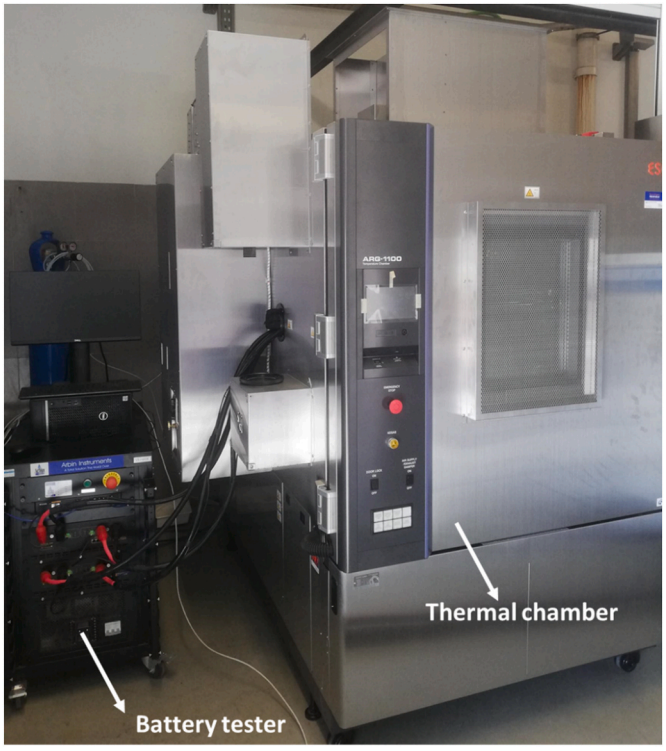

Fig. 1. Test bench for battery cell characterization.

They found that the most suitable model for LFP and NCA chemistries was a first order ECM with hysteresis, whereas the best for NMC and LMO chemistries was a first order ECM without hysteresis. Yamanaka et al. [31] proposed a multi-physics equivalent circuit model for an entire battery pack. Starting from the ECM of a single cell, and suitably connecting the cells in series and in parallel, they obtained the ECM of the entire battery pack. Lai et al. [13] introduced a parameter sensitivity analysis in order to improve the accuracy of equivalent circuit models. They considered a second order ECM with hysteresis and the sensitivity analysis results were used to reduce the look-up tables of the different model parameters. They found that not all the second order ECM parameters needed to be updated with respect to the state of charge as the model precision is not significantly affected by this reduction in the look-up tables. Huang et al. [14] studied equivalent circuit models aimed at the prediction of the electric behavior of electric vehicle batteries. They compared four types of equivalent circuit models (Rint, Thevenin, second order ECM and PNGV) and they found that the PNGV model was the most suitable for this kind of application, with an average terminal voltage error of almost 5 mV. Tran et al. [15] proposed a comprehensive equivalent circuit model incorporating the effects of state of health, state of charge and temperature on the model parameters. In spite of providing a very detailed description of the electric behavior of the lithium-ion cells, this methodology needs an extensive experimental characterization and the look-up tables of the electrical parameters provided to the model are specific for the tested cell.

A usual protocol for obtaining such look-up tables is the Hybrid Power Pulse Characterization Test (HPPC) which allows to determine electrical parameters by testing the cell with charge/discharge pulses at different state of charge and c-rates [16]. This means that the use of an ECM for a particular cell requires a certain amount of testing time.

As a result, most of the equivalent circuit models available in the literature can be applied only to the particular cell for which they were developed. Considering instead a cell with the same chemistry but with different format, volume, or capacity, implies additional testing to identify its specific electrical parameters. Therefore, a model that could be applied to a family of cells without the need of further testing would be very desirable.

In the literature, only a few authors have proposed models that might be applied to a family of cells, and not only to a specific cell experimentally characterized. Freudiger et al. [17] proposed a generalized equivalent circuit model based on a regression model. By using data depending on the chemistry (volumetric and gravimetric energy and power densities) the internal resistance and other electrical parameters were expressed in terms of the previously mentioned chemistry parameters. This model was generalized to five different chemistries and only to cylindrical cells. The advantage is that a generalized model for all the chemistry was provided, but the drawback is that the regression model had no physical basis, as it was based only on the regression models provided by MATLAB's Regression Learner Toolbox in order to extract the coefficient for each chemistry. Zhang et al. [18] proposed a generalized SOC-OCV model for lithium-ion batteries that allows to estimate the open circuit voltage of different types of lithium-ion batteries. Nevertheless, the authors did not explore any generalized model for the internal resistance of lithium-ion cells.

Table 4
LFP cells data found in the literature.

Cell number	Capacity [Ah]	Nominal Voltage [V]	Minimum Voltage [V]	Maximum Voltage [V]	Format
6	16	3.2	2.5	4.2	Cylindrical
7	40	3.2	2.5	4.2	Pouch
8	42	3.2	2.5	4.2	Pouch
9	60	3.2	2.5	4.2	Prismatic

Table 3
LFP cells tested in-house.

Cell number	Capacity [Ah]	Nominal Voltage [V]	Minimum Voltage [V]	Maximum Voltage [V]	Format	Dimensions [mm^3]
1	1.8	3.2	2.5	4.2	Cylindrical	18650
2	3.8	3.2	2.5	4.2	Cylindrical	26650
3	6	3.2	2.5	4.2	Cylindrical	32700
4	70	3.2	2.5	4.2	Prismatic	173 × 97 × 40
5	100	3.2	2.5	4.2	Prismatic	173 × 207 × 28

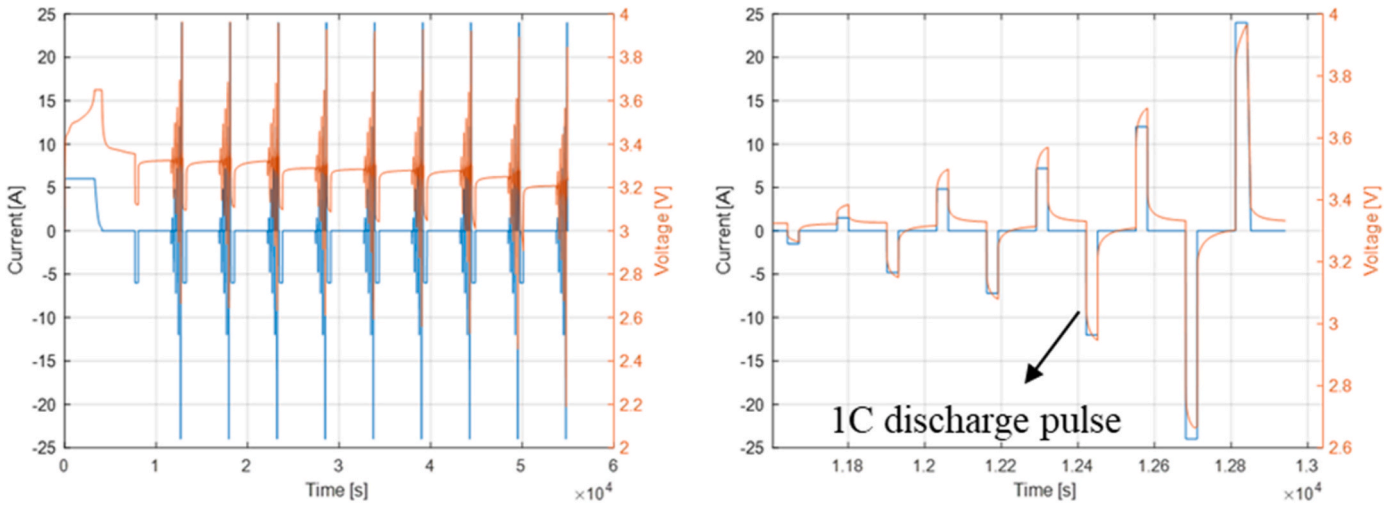

Fig. 2. HPPC test profile (left); customizable pulse sequence (right).

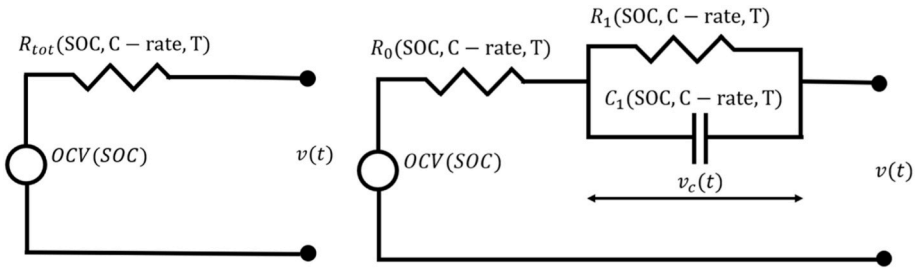

Fig. 3. 0[th]-order ECM (left), 1st-order ECM (right).

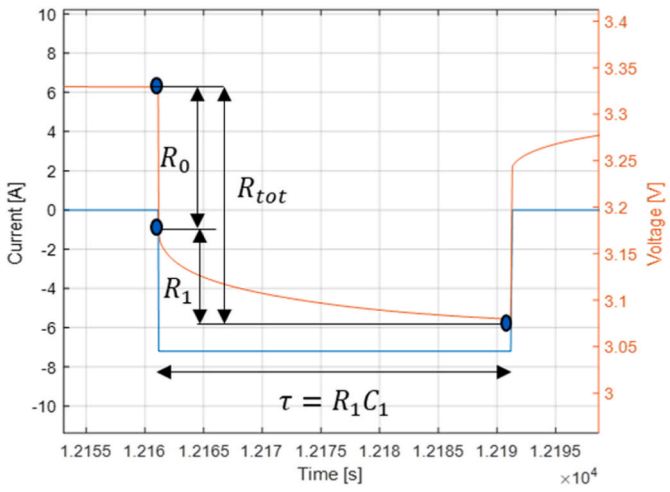

Fig. 4. Step method visualization.

This work is aimed at providing a generalized equivalent circuit model for LFP chemistry that, once developed and calibrated, should provide a description of the electrical behavior of any cell belonging to the LFP category. The model is based on a physical relationship between the nominal capacity available in the datasheet and the internal resistance of the lithium-ion cell. The proposed internal resistance model relies only on one tuning parameter, the chemistry characteristic coefficient, that is the same for all the cells belonging to the LFP category. This chemistry characteristic coefficient has an Arrhenius-like trend with respect to temperature, which is physically meaningful because the same kind of trend is typical of the dependence with respect to temperature of the internal resistance of lithium-ion cells. In order to calibrate this model, data collected from the testing of five LFP cells were considered. Other data from the literature were included in order to build a larger dataset and to confirm the results obtained with the cells tested in-house. This model generates two main advantages:

- First, every lithium-iron phosphate cell could be described by knowing only its capacity (provided in the cell datasheet) and the operating temperature. This led to considerable savings of time (the characterization of a lithium-ion cell implies several HPPC tests repeated at different temperatures in order to build-up the look-up tables).
- Secondly, by employing this model, the realization of a specific test bench for lithium-ion cells (which would comprise a battery tester, a climatic chamber, recording equipment and temperature sensors) might be avoided. This could be particularly useful for all the operators who need a precise estimation of the electrical behavior and heat generation of an LFP cell, without having any specific test bench to test it.

Of course, the methodology shown in this paper could be applied to other chemistries in the future, and in this way, generalized equivalent circuit models for each of the main LIBs technologies on the market would be available. The model proposed is validated by using an extremely dynamic real driving cycle both for a low-capacity cell (cylindrical cell) and for a high-capacity cell (prismatic cell) and finally the errors are compared to those obtained by using a specific first order ECM calibrated for the cells used in the validation process.

The paper is structured into five sections: after this introduction, in section 2 the cell under analysis is described and the experimental test bench used for collecting the data is illustrated. In section 3, the results of the experimental characterization for the different cells are shown,

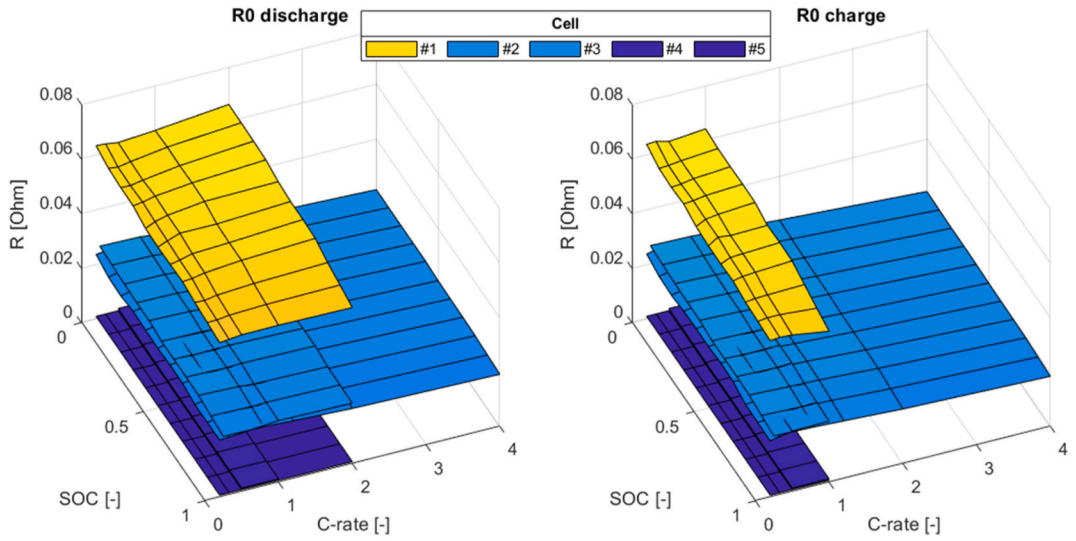

Fig. 5. Ohmic resistance at 20 °C for the tested cells.

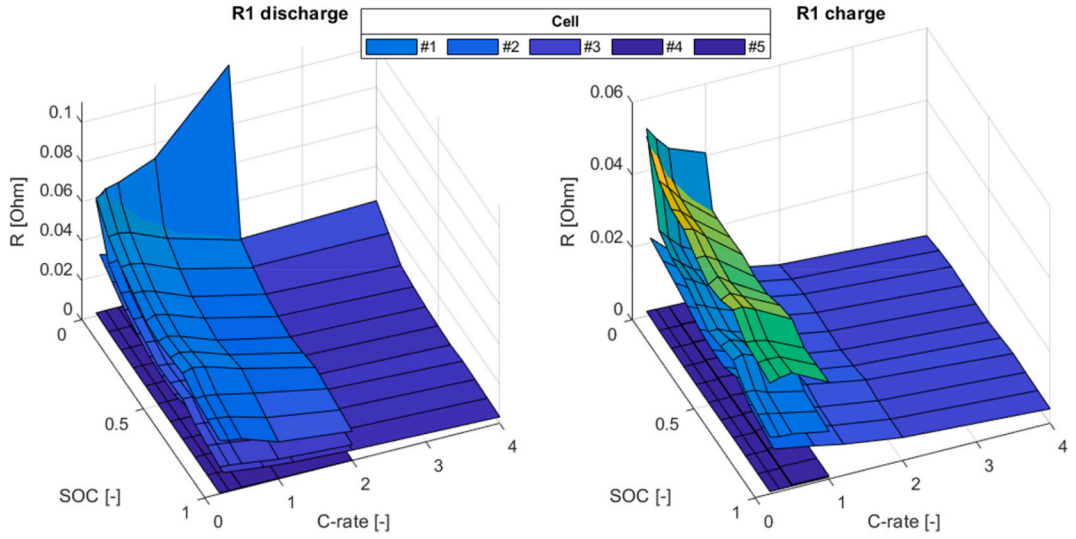

Fig. 6. Charge transfer resistance at 20 °C for the tested cells.

whereas in section 4 the model development and implementation are described. Finally, in section 5 the model validation is provided for low and high-capacity cells and in section 6 the conclusions are pointed out.

2. Experimental test bench

The data used for the implementation of this generalized model have been collected through a large experimental characterization campaign. The test bench used for lithium-ion cells testing relies on an Arbin battery tester, which allows to charge/discharge cells with high voltage resolution ($\sim$ 1 μV) and very good voltage and current accuracies ($\pm$ 2 mV and $\pm$ 20 mA, respectively). The cells are tested inside a climatic chamber whose characteristics are listed in Table 1. The cells are equipped with K-type thermocouples in order to measure the temperature evolution and all the data are recorded with a datalogger. The uncertainties in the measurement of electrical current, voltage and temperature are listed in Table 2. The thermal chamber and the battery tester can be observed in Fig. 1.

3. Experimental characterization of the lithium-ion cells

Five LFP cells were experimentally characterized and the data collected from the testing protocols were used both for implementing specific equivalent circuit models for each one of these cells, and for generating the generalized ECM for LFP cells. The characteristics of the cells used are listed in Table 3.

Additionally to these cells, other cells whose data were available in the literature were considered in the analysis, in order to get a broader and more general view on the problem. The characteristics of these additional cells are listed in Table 4 [19,20].

In order to determine the electrical parameters specific to each of the tested cells (see Table 3), tests performed according to the HPPC protocol were carried out at several temperatures. This protocol consists of a sequence of charge/discharge pulses which are customized for each tested cell according to their charge/discharge rate limits. As an example, the HPPC protocol is shown in Fig. 2 for cell #3 together with a zoom on the customizable pulse train which is usually designed for multi-rate analysis.

In the HPPC test profile, the customizable pulse sequence is repeated 9 times, and it is followed by a discharge of 10 % of the cell capacity.

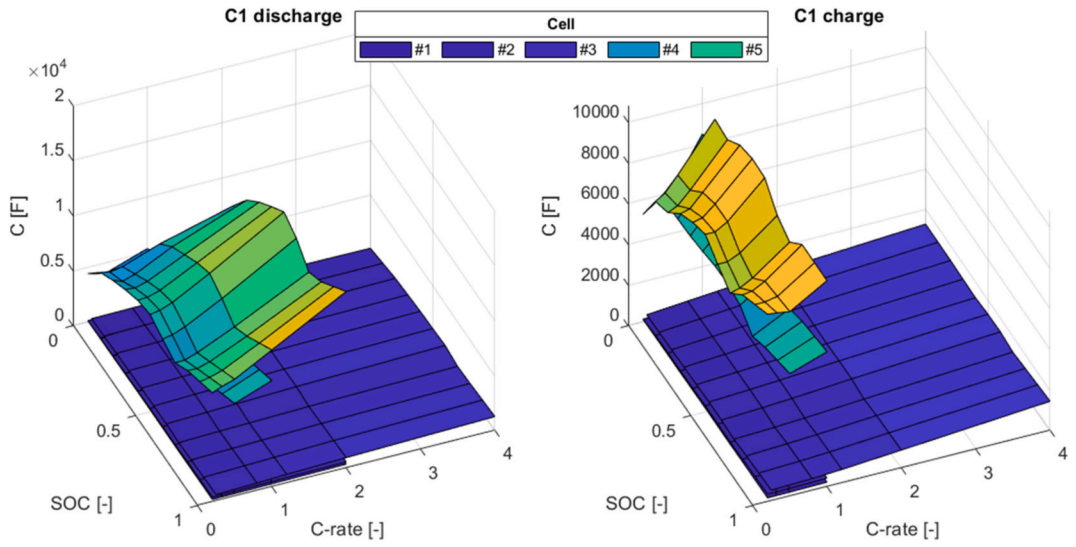

Fig. 7. Double-layer capacitance at 20 °C for the tested cells.

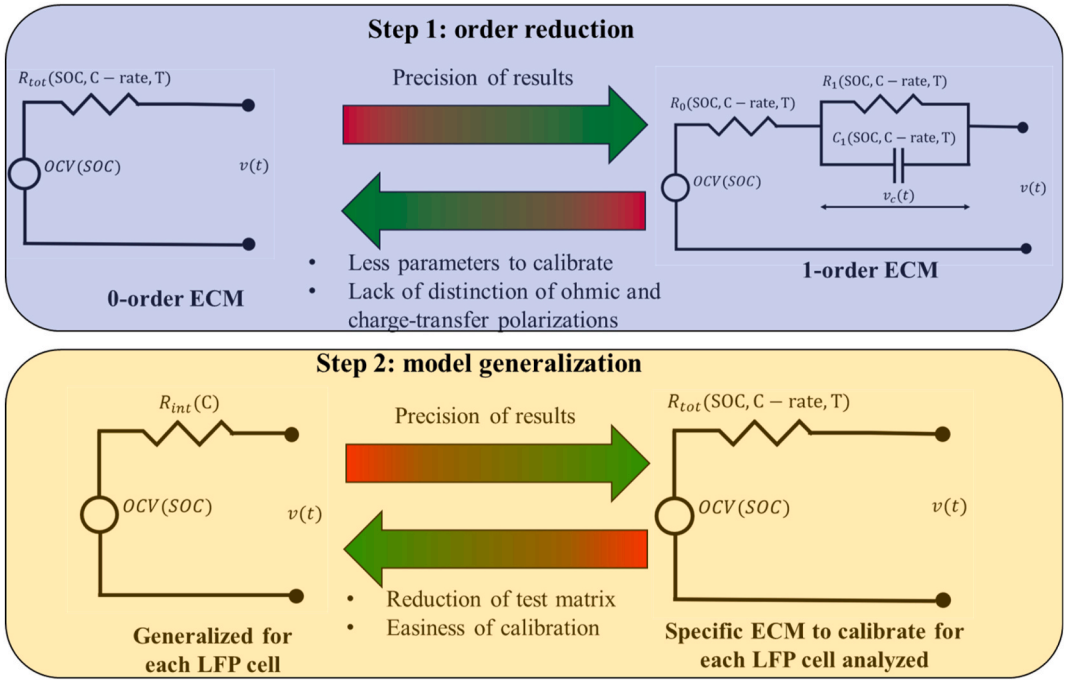

Fig. 8. Steps for model development.

This is done to calibrate the electrical parameters at several stages of the state of charge from SOC = 0.9 to SOC = 0.1. Finally, the HPPC test is repeated at several temperatures (0, 10, 20 and 30 °C) to consider the impact of the temperature on the electrical parameters.

Once all the tests were executed, in order to extract the electrical parameters for the implementation of equivalent circuit models, a step method is employed. Depending on whether it is a 0^{th}-order or a 1st-order model (see Fig. 3), the parameters to be determined differ: for a 0^{th}-order model only the total resistance (R_{tot}) needs to be determined, whereas for a 1st-order model the ohmic resistance (R_0) is determined through the drop in instantaneous voltage, while the resistance due to charge transfer (R_1) and the double-layer capacitance (C_1) are determined by fitting the difference to an exponential curve as shown in Fig. 4 [21].

In this way, maps of the electrical parameters can be obtained for each of the tested cells. The maps of the electrical parameters are presented in Figs. 5–7 only for the case of room temperature (T = 20 °C).

As explained by Broatch et al. [22], these maps are usually given as three-dimensional maps considering state of charge, c-rate and temperature dependencies. This huge amount of data is extracted by several tests which takes a long time, both for execution and post-processing. Furthermore, for each cell, a different and specific equivalent circuit model needs to be calibrated, which will give information only on that specific cell.

Starting from this consideration, a generalized ECM model for LFP chemistries would be a novelty to the current literature, because it would provide a tool that could describe the behavior of all the cells belonging to this category, generating great savings of time and resources (operative time and work, test bench design and implementation, post-processing software licenses, etc.).

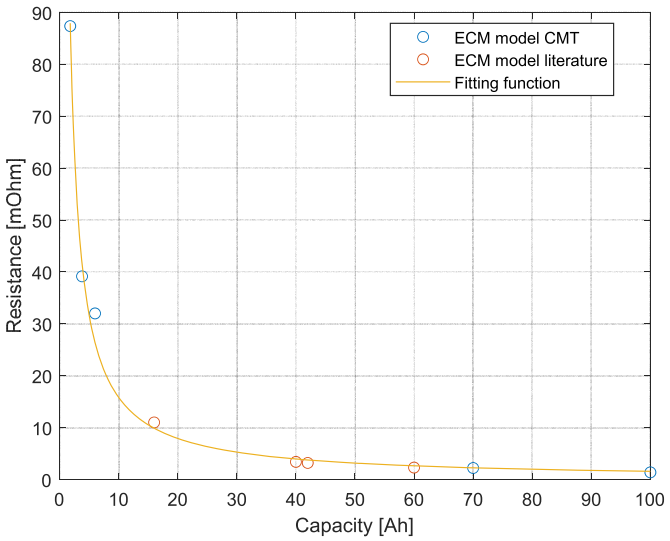

Fig. 9. Internal resistance at 20 °C against the nominal capacity of the analyzed cells, measured and modeled data.

4. Model development and implementation

The logical steps followed in the development of the generalized LFP model are shown in Fig. 8, in which two main steps can be found:

- 1st step: order reduction. Going from the 1st-order model to the 0^{th}-order model, the estimation of the terminal voltage will be less precise since a 0^{th}-order model does not consider the dynamic behavior of the battery when an electric current is applied [23]. On the other hand, in a 0^{th}-order model one only needs to calibrate a total resistive parameter, whereas the calibration process of a 1st-order model is more complicated because the charge-transfer resistance and the double-layer capacitance are obtained as a result of the fitting to the voltage drop during a pulse. Nevertheless, the test matrix is still the same for the two models and thus there is no reduction of the testing time because the parameters of the two models need to be calibrated in all the different charge/discharge rate, state of charge and temperature conditions within the safe operating area of each of the cells. Finally, one must test each cell to calibrate its specific electrical parameters: for instance, one would need to calibrate five ECMs for the five LFP cells considered here.
- 2nd step: model generalization. Going from the specific ECM for each cell to the generalized LFP cell model, it is expected to lose some precision in the results since, in the generalized model, no look-up table is provided, and the resistance is not obtained from maps depending on the abovementioned stress factors (SOC, c-rate and temperature), but the generalized internal resistive parameter will be dependent only on the nominal capacity of the cell, which can be found in the datasheet. This second step, differently from the previous one, leads to a considerable reduction in the test matrix needed for the model implementation and to a simplification of the calibration process. The generalized model, in fact, relies only on a

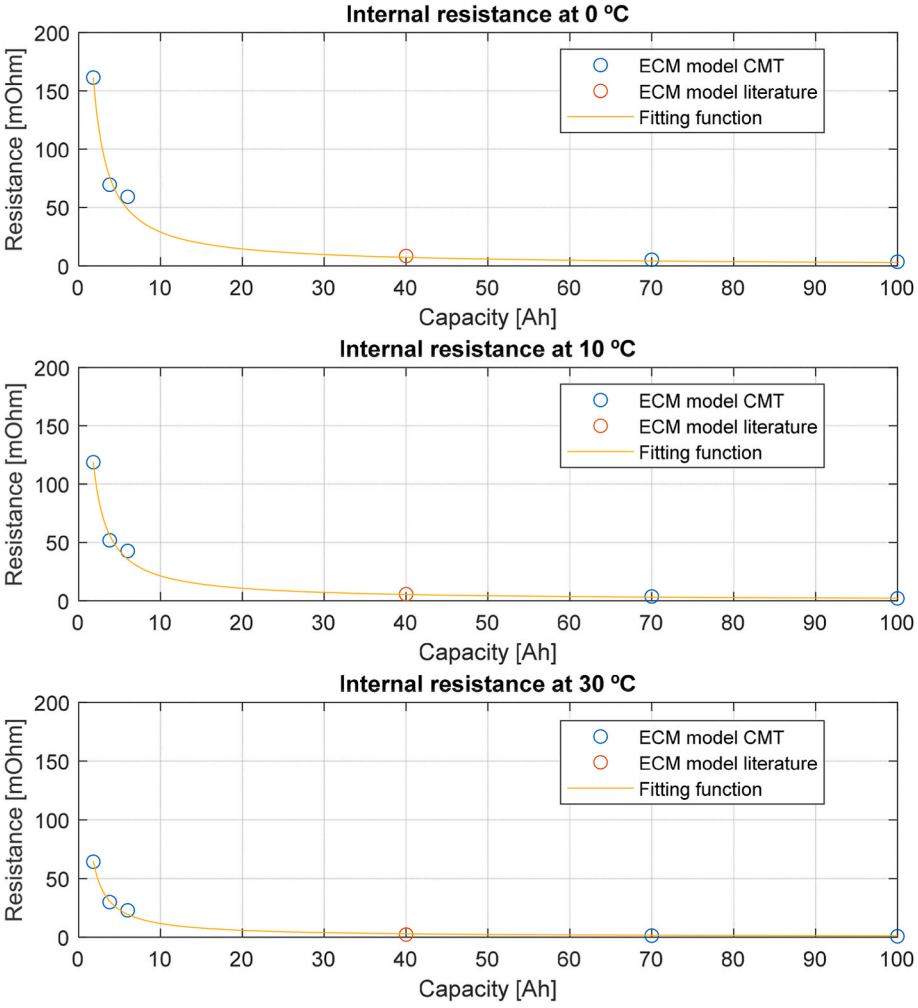

Fig. 10. Internal resistance at 0, 10 and 30 °C against the nominal capacity of the analyzed cells: measured and modeled data.

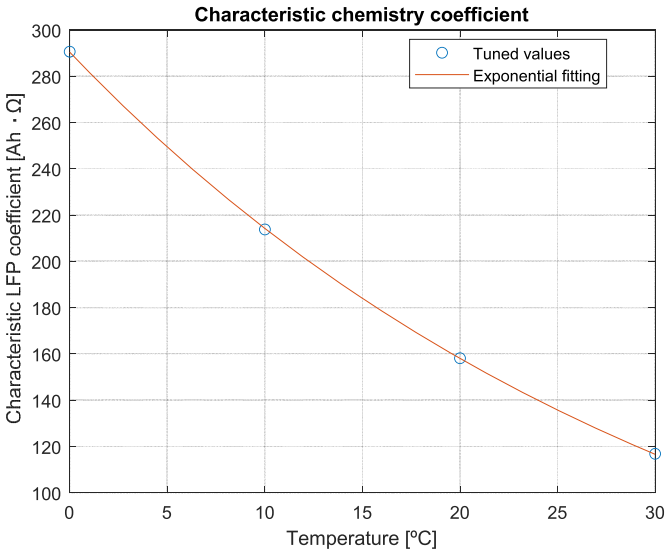

Fig. 11. Characteristic chemistry coefficient vs temperature: values obtained from data evaluation and exponential fitting.

correlation of the internal resistance with respect to the nominal capacity of the cell.

In order to find out a generalized correlation of the internal resistance of a lithium-ion cell with respect of the nominal capacity, the following assumptions can be considered:

- The internal electrical resistance of a lithium-ion cell can be expressed as in Equation (1):

$$R_{int} = \frac{\rho_{el} L_{current}}{A} \tag{1}$$

where ρ_{el} is the electrical resistivity of the cell, A is the area through which the electrical current is flowing and $L_{current}$ represents the path followed by the current between the two electrodes, which is strongly affected by format, geometry and also the manufacturing characteristics of the cell, as shown by Lee et al. [24].

- Additionally, the capacity of a cell, which is the energy that can be stored in a cell, can be expressed as in Equation (2):

$$C = V_{current} E_d = A L_{current} E_d \tag{2}$$

where E_d stands for the energy density of the cell expressed in Ah.

From Equations (1) and (2), it is readily obtained that:

$$R_{int} = \frac{1}{C}\left[\rho_{el} E_d (L_{current})^2\right] = \frac{k_{LFP}}{C} \tag{3}$$

From Equation (3), an inverse proportionality between internal resistance of the cell and its capacity is found. Furthermore, the found correlation gives some insight on where this proportionality comes from. In this work, the coefficient k_{LFP} is defined as a characteristic chemistry coefficient because, once it is determined, it is a constant and it can provide the values of internal resistance for each cell belonging to the LFP category, once its nominal capacity is known. Since a physical-based correlation of the internal resistance with respect of the capacity is theoretically found, it is reasonable to expect that the experimental data collected for the different LFP cells will confirm Equation (3). As well as for the maps of the first order model presented in Figs. 5–7, also for the zeroth order model, similar maps of the total internal resistance can be obtained with respect to the state of charge, c-rate and temperature. From the maps of the total internal resistance, it is possible to obtain the curve plotted in Fig. 9, which represents the internal resistance of the cell in the reference condition equal to SOC = 50 %, 1C and at 20 °C. From Fig. 9, it is possible to find out the relation between the internal resistance of the cell, obtained from the testing characterization and from the data of the cells selected in the literature, and the nominal capacity of the cell, available in the datasheet. It is confirmed that the internal resistance of the cell has an inverse relationship with respect to the nominal capacity. In fact, the model shows very good agreement

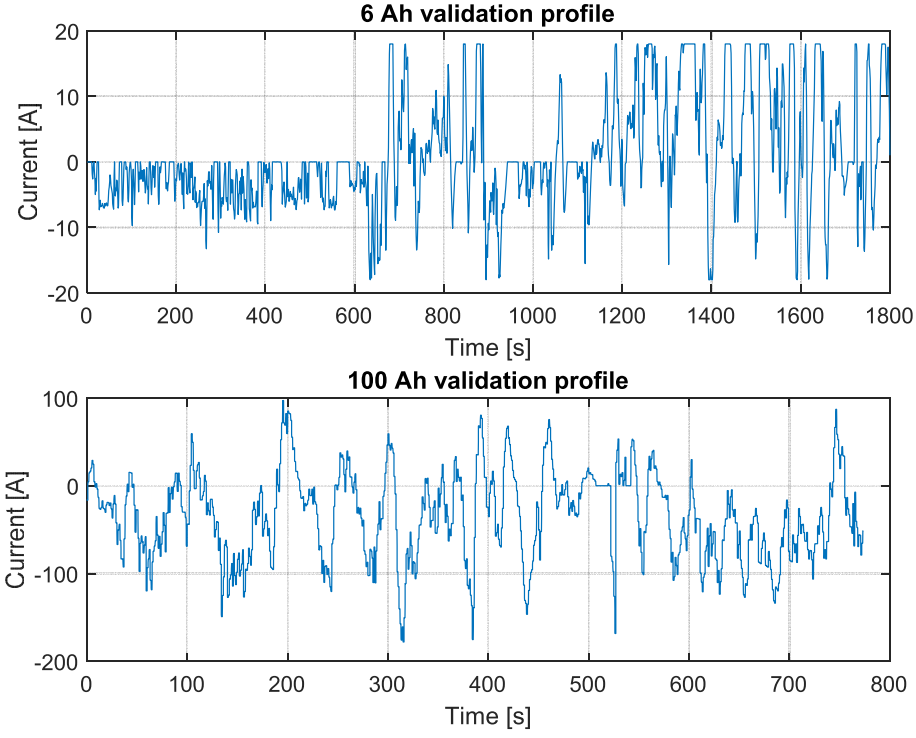

Fig. 12. Validation profiles for a low-capacity and a high-capacity LFP cell.

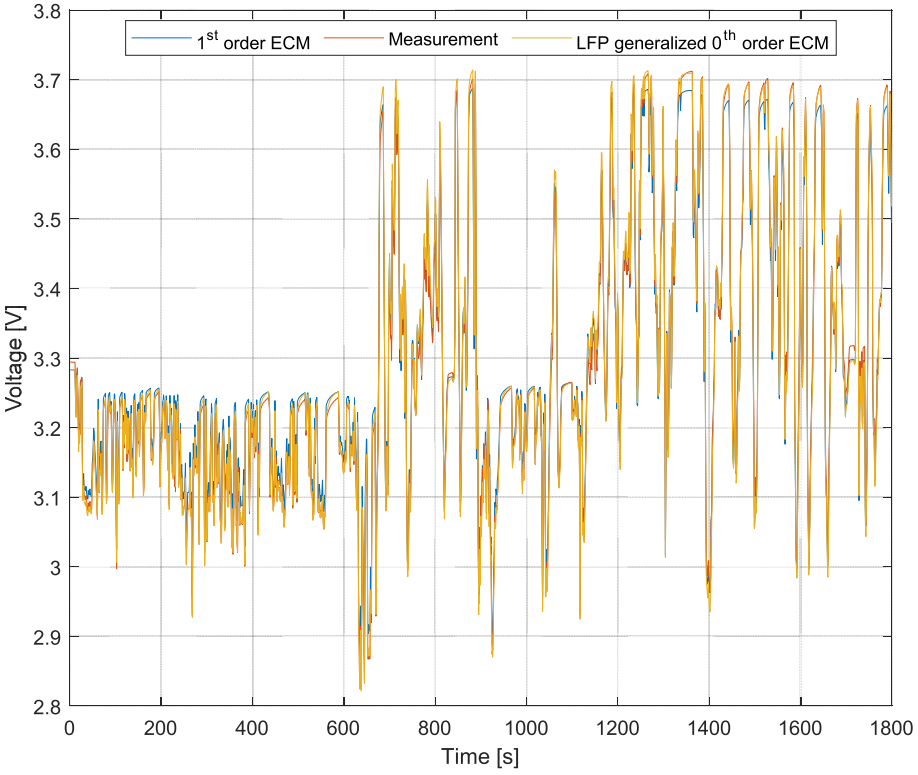

Fig. 13. Validation of the generalized electrical model for the cylindrical 6 Ah cell compared to the specific 1st-order model.

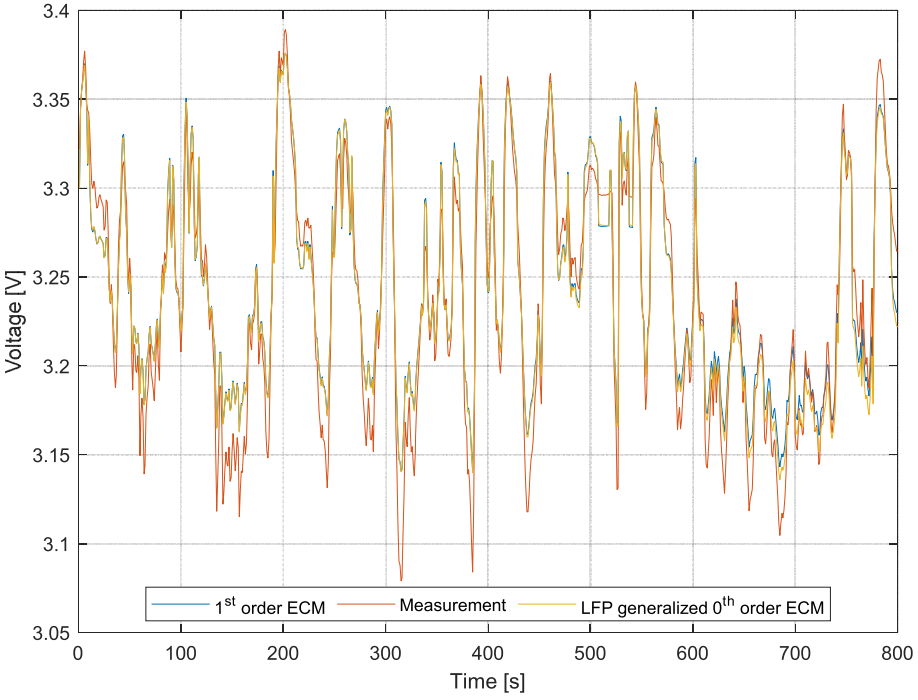

Fig. 14. Validation of the generalized electrical model for the prismatic 100 Ah cell compared to the specific 1st-order model.

with the experimental data at 20 °C and a characteristic chemistry coefficient $k_{LFP} = 160$ AhΩ is found.

The model developed so far does not take into account the dependency on temperature, which actually cannot be neglected. In fact, it is well demonstrated in previous work that the resistive parameters of a lithium-ion cell exhibit an Arrhenius-like dependence on temperature: as it gets higher, the resistance of the cell decreases, following an inverse exponential curve. Therefore, in order to consider also this aspect, data were collected for the tested cells at other 3 temperatures (0, 10 and 30 °C). These data are represented in Fig. 10.

The results at different temperatures show good agreement with the experimental data as in the standard temperature case. The characteristic chemistry coefficient values obtained from the previous optimization for the four different testing temperatures is shown in Fig. 11. The

Table 5
Root mean square errors obtained with a specific 1st order and a generalized 0th order model for a low-capacity and a high-capacity cell.

LFP cell	Specific 1st-order ECM	Generalized 0th-order ECM
6 Ah cylindrical cell	1.07%	1.33%
100 Ah prismatic cell	1.31%	1.59%

tuned values obtained from the previous optimization clearly show an Arrhenius-like tendency, which can be expressed as in Equation (4):

$$k_{LFP} = k_0 \exp\left(-\frac{E_a}{RT}\right) \tag{4}$$

In Equation (4), k_0 is a pre-exponential factor and E_a is the activation energy, which are the typical tuning parameters of an Arrhenius-like dependency. The same functional dependency on the temperature is widely used in order to explain the change of internal cell resistance under a change in the temperature [25,26].

This physically plausible expression of the characteristic chemistry coefficient can thus be implemented in the final model, which is expressed in Equation (5):

$$R_{int} = f(C,T) = \frac{1}{C} k_0 \exp\left(-\frac{E_a}{RT}\right) \tag{5}$$

The model expressed in Equation (5) describes the electrical behavior of all the cells belonging to the LFP category and their change with respect to the temperature. In section 5, this model is validated for a low-capacity and a high-capacity LFP cell in order to test its quality and to compare its precision with that of a specific 1st-order ECM developed for the cells considered.

5. Model validation for a low-capacity and a high-capacity cell

For the validation of the generalized LFP cell model, multi-rate dynamic profiles have been used. These profiles are generated in-house and scaled according to the rate limits and capacities of the cells to test. The low-capacity cell used for this validation is a 6 Ah cylindrical cell, whose charge/discharge limits are 3C: therefore, the current profile shows peaks up to 18 A. On the other hand, the high-capacity cell is a 100 Ah prismatic cell, whose charge limit is equal to 1C (100 A) and the discharge limit is equal to 2C (200 A).

These current profiles are implemented in the software that controls the battery tester as text files: the battery tester charges/discharges the cells according to the specific current profile with a time-step of 1 s (see Fig. 12). The voltage is measured by the battery tester and it is compared to the modeled terminal voltage obtained by simulating the cell with a previously validated and specific 1st-order model (best available model for those cells) and with the generalized LFP model. The results of the validation process are shown in Figs. 13 and 14 for both the cells analyzed. The root mean square errors are listed in Table 5.

As expected, the specific 1st-order model provides better results for both cells as, in fact, it uses three-dimensional look-up tables of the electrical parameters which perfectly describe their changes with respect to the state of charge, c-rate and temperature. Nevertheless, the calibration of these parameters requires extensive experimental work. Conversely, the generalized LFP model, which relies only on the nominal capacity of the cell as found in the datasheet, and that considers the temperature variation through a simple Arrhenius function calibrated for the generalized model, also provides good results. In fact, the error

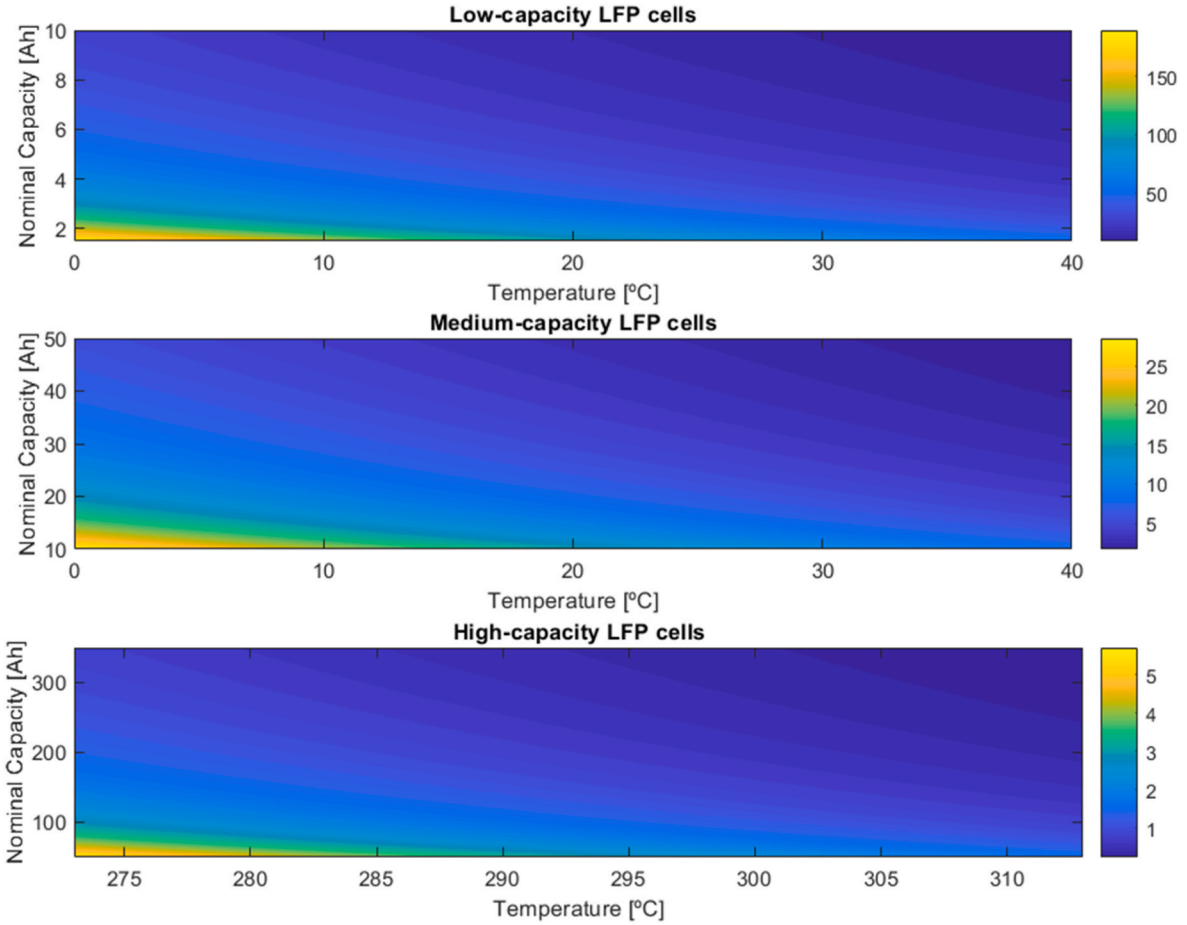

Fig. 15. Internal resistance maps built with the generalized LFP model.

provided by the generalized model is lower than 2 % for both cells and it may be considered validated and thus useable for LFP cells analyses.

From this model, a map representing the global behavior of LFP cells was constructed. Considering a usual temperature operating range from 0 to 40 $^{\circ}C$, and cells ranging from 1.5 Ah (very low capacity for a cylindrical cell) to 350 Ah (very large for a prismatic cell), the map shown in Fig. 15 was generated. Considering the change of several orders of magnitude between the internal resistance of low-capacity cells and very large prismatic cells, it was decided to produce 3 maps: for low-capacity cells [27] (up to 10 Ah), for medium-capacity cells [28] (up to 50 Ah) and for high-capacity cells [29] (up to 350 Ah), in order to gain some resolution in data representation. These maps may be used both for off-line studies, such as estimation of the electrical behavior, and calculation of the heat generation of the cells under different operating and environmental conditions, and for on-line applications as in on-board BMS control algorithms for state of charge and state of health estimation [30].

6. Conclusions

A generalized LFP equivalent circuit model was proposed. The main conclusions can be summarized as follows:

- The advantages of such a methodology consist in providing a numerical tool capable of describing the electrical behavior of all cells belonging to the LFP category, thus reducing significantly the testing matrix and the testing time.
- The model only needs the nominal capacity and provides the values of internal resistance for the chosen cells. An inverse proportionality was found between the nominal capacity of the cells and their internal resistance. The model is physically plausible and only one tuning parameter needs to be determined.
- A characteristic chemistry coefficient was defined and its dependency on temperature was found to be Arrhenius-like. This tendency is physically plausible since cell resistance decreases exponentially with the temperature.
- The model was validated both for a low-capacity cylindrical cell and for a high-capacity prismatic cell providing errors below 2 %.
- Maps of the internal resistance can be produced and subsequently integrated into control strategies of battery management systems for state of charge and state of health estimation, or they can be used for off-line analyses.

Declaration of competing interest

The authors declare that they have no known competing financial interests or personal relationships that could have appeared to influence the work reported in this paper.

Data availability

The data that has been used is confidential.

Acknowledgments

This work was supported by Generalitat Valenciana within the framework of the PROMETEO project “Contribution to the decarbonization of transport by optimizing the thermal management of vehicle batteries electrified” with reference number PROMETEO/2020/042. Luca Agizza is supported by grant ACIF/2021/005 funded by Conselleria de Innovación, Universidades, Ciencia y Sociedad Digital of the Generalitat Valenciana. A special thanks goes to Eng. Bernardo Planells Vela for his valuable effort in realizing all the experiments needed for this work and for the preparation of the test-bench.

References

[1] Olabi AG, Abbas Q, Shinde PA, Abdelkareem MA. Rechargeable batteries: technological advancement, challenges, current and emerging applications. Energy 2022:126408.
[2] Armand M, Axmann P, Bresser D, Copley M, Edström K, Ekberg C, Guyomard D, Lestriez B, Novak P, Petranikova M, Porcher W, Trabesinger S, Wohlfahrt-Mehrens M, Zhang H. Lithium-ion batteries - current state of the art and anticipated developments. J Power Sources 2020;479:228708.
[3] Lyu P, Liu X, Qu J, Zhao J, Huo Y, Qu Z, Rao Z. Recent advances of thermal safety of lithium ion battery for energy storage. Energy Storage Mater 2020;31:195–220.
[4] Tran MK, Mevawalla A, Aziz A, Panchal S, Xie Y, Fowler M. A review of lithium-ion battery thermal runaway modeling and diagnosis approaches. Processes 2022;10 (6):1192.
[5] Piao N, Gao X, Yang H, Guo Z, Hu G, Cheng HM, Li F. Challenges and development of lithium-ion batteries for low temperature environments. eTransportation 2022; 11:100145.
[6] Chen Y, Kang Y, Zhao Y, Wang L, Liu J, Li Y, Liang Z, He X, Li X, Tavajohi N, Li B. A review of lithium-ion battery safety concerns: the issues, strategies, and testing standards. J Energy Chem 2021;59:83–99.
[7] Han X, Lu L, Zheng Y, Feng X, Li Z, Li J, Ouyang M. A review on the key issues of the lithium ion battery degradation among the whole life cycle. eTransportation 2019;1:100005.
[8] Wu C, Sun J, Zhu C, Ge Y, Zhao Y. Research on overcharge and overdischarge effect on lithium-ion batteries. In: 2015 IEEE vehicle power and propulsion conference (VPPC). IEEE; 2015. p. 1–6.
[9] Gao Y, Zhu C, Zhang X, Guo B. Implementation and evaluation of a practical electrochemical-thermal model of lithium-ion batteries for EV battery management system. Energy 2021;221:119688.
[10] Kang D, Lee PY, Yoo K, Kim J. Internal thermal network model-based inner temperature distribution of high-power lithium-ion battery packs with different shapes for thermal management. J Energy Storage 2020;27:101017.
[11] Samieian MA, Hales A, Patel Y. A novel experimental technique for use in fast parameterisation of equivalent circuit models for lithium-ion batteries. Batteries 2022;8(9):125.
[12] Tran MK, DaCosta A, Mevawalla A, Panchal S, Fowler M. Comparative study of equivalent circuit models performance in four common lithium-ion batteries: LFP, NMC, LMO, NCA. Batteries 2021;7(3):51.
[13] Lai X, Meng Z, Wang S, Han X, Zhou L, Sun T, Li X, Wang X, Ma Y, Zheng Y. Global parametric sensitivity analysis of equivalent circuit model based on Sobol’method for lithium-ion batteries in electric vehicles. J Clean Prod 2021;294:126246.
[14] Huang H, Wang Y, Wang H. Research on parameter identification of lithium battery equivalent circuit model based on recursive gradient correction algorithm. In: Proceedings of the 16th annual conference of China electrotechnical society, vol. III. Singapore: Springer Nature Singapore; 2022. p. 153–61.
[15] Tran MK, Mathew M, Janhunen S, Panchal S, Raahemifar K, Fraser R, Fowler M. A comprehensive equivalent circuit model for lithium-ion batteries, incorporating the effects of state of health, state of charge, and temperature on model parameters. J Energy Storage 2021;43:103252.
[16] Pan D, Guo H, Tang S, Li X, Wang Z, Peng W, Wang J, Yan G. Evaluating the accuracy of electro-thermal coupling model in lithium-ion battery via altering internal resistance acquisition methods. J Power Sources 2020;463:228174.
[17] Freudiger D, D’Arpino M, Canova M. A generalized equivalent circuit model for design exploration of li-ion battery packs using data analytics. IFAC-PapersOnLine 2019;52(5):568–73.
[18] Zhang C, Jiang J, Zhang L, Liu S, Wang L, Loh PC. A generalized SOC-OCV model for lithium-ion batteries and the SOC estimation for LNMCO battery. Energies 2016;9(11):900.
[19] Anseán D, González M, Viera JC, Garcia VM, Alvarez JC, Blanco C. Electric vehicle Li-Ion battery evaluation based on internal resistance analysis. In: 2014 IEEE vehicle power and propulsion conference (VPPC). IEEE; 2014. p. 1–6.
[20] Lin C, Xu S, Liu J. Measurement of heat generation in a 40 Ah LiFePO4 prismatic battery using accelerating rate calorimetry. Int J Hydrogen Energy 2018;43(17): 8375–84.
[21] Farmann A, Sauer DU. A comprehensive review of on-board State-of-Available-Power prediction techniques for lithium-ion batteries in electric vehicles. J Power Sources 2016;329:123–37.
[22] Broatch A, Olmeda P, Margot X, Agizza L. A generalized methodology for lithium-ion cells characterization and lumped electro-thermal modelling. Appl Therm Eng 2022;217:119174.
[23] He X, Sun B, Zhang W, Fan X, Su X, Ruan H. Multi-time scale variable-order equivalent circuit model for virtual battery considering initial polarization condition of lithium-ion battery. Energy 2022;244:123084.
[24] Lee KJ, Smith K, Pesaran A, Kim GH. Three dimensional thermal-, electrical-, and electrochemical-coupled model for cylindrical wound large format lithium-ion batteries. J Power Sources 2013;241:20–32.
[25] Berrueta A, Urtasun A, Ursúa A, Sanchis P. A comprehensive model for lithium-ion batteries: from the physical principles to an electrical model. Energy 2018;144: 286–300.
[26] Bensaad Y, Friedrichs F, Baumhöfer T, Eswein M, Bähr J, Fill A, Birke KP. Embedded real-time fractional-order equivalent circuit model for internal resistance estimation of lithium-ion cells. J Energy Storage 2023;67:107516.
[27] Jia Z, Huang Z, Zhai H, Qin P, Zhang Y, Li Y, Wang Q. Experimental investigation on thermal runaway propagation of 18,650 lithium-ion battery modules with two cathode materials at low pressure. Energy 2022;251:123925.

[28] Huang Z, Li X, Wang Q, Duan Q, Li Y, Li L, Wang Q. Experimental investigation on thermal runaway propagation of large format lithium ion battery modules with two cathodes. Int J Heat Mass Tran 2021;172:121077.
[29] Dondelewski O, O'Connor TS, Zhao Y, Hunt IA, Holland A, Hales A, Offer GJ, Patel Y. The role of cell geometry when selecting tab or surface cooling to minimise cell degradation. eTransportation 2020;5:100073.
[30] Meng J, Luo G, Ricco M, Swierczynski M, Stroe DI, Teodorescu R. Overview of lithium-ion battery modeling methods for state-of-charge estimation in electrical vehicles. Appl Sci 2018;8(5):659.
[31] Yamanaka T, Kihara D, Takagishi Y, Yamaue T. Multi-physics equivalent circuit models for a cooling system of a lithium ion battery pack. Batteries 2020;6(3):44.
[32] Thakkar RR. Electrical equivalent circuit models of lithium-ion battery. Manag Appl Energy Storage Dev 2021:3–10.